Experimental Two-Photon, Three-Dimensional Entanglement for Quantum Communication

Alipasha Vaziri,[1] Gregor Weihs,[1,2] and Anton Zeilinger[1]

[1]*Institut für Experimentalphysik, Universität Wien, Boltzmanngasse 5, A-1090 Wien, Austria*

[2]*Ginzton Laboratory, S-23, Stanford University, Stanford, California 94304*

(Received 21 June 2002; published 20 November 2002)

Orbital angular momentum entangled photons emitted by a down-conversion source are in higher dimensional entangled states. Here we report the experimental confirmation by demonstrating a violation of a generalized Clauser-Horne-Shimony-Holt–type Bell inequality in three dimensions by more than 18 standard deviations. Higher dimensional entangled states allow the realization of new types of quantum communication protocols. They also provide a more secure quantum cryptography scheme. Therefore our experimental results are likely to have applications in future quantum communication technology.

DOI: 10.1103/PhysRevLett.89.240401 PACS numbers: 03.65.Ud, 03.67.Hk, 42.50.Gy

Triggered by research in the foundations of quantum mechanics, in more recent years new ways of computation and communication were discovered, where entanglement plays a central role. Various quantum information protocols require the use of more complicated entanglement than the common entanglement between two particles, each one defined effectively in two dimensions, i.e., two qubits [1]. This includes certain schemes of quantum cryptography, quantum teleportation, and proposals for quantum computers [2–4]. Until recently, nearly all of the theoretical discussion and certainly all experiments focused on the use of qubits including the generalization to three or more two-dimensional entangled qubits [5–9]. Most recently, novel schemes were proposed, necessitating the use of qutrits for higher dimensional entangled systems [10–13], which still await experimental verification. One should mention that, in principle, qutrits could be realized by a generalization of the Franson scheme, exploiting energy-time entanglement [14]. Another possibility is to exploit correlations between more than two qubits to obtain qutrit entanglement as demonstrated by Howell *et al.* [9]. Yet it is obviously preferable if the qutrits were carried by one particle in one spatial mode.

Given the high technical status of photonic technology and the fact that photons will for a long time remain the only means for quantum communication, it is desirable to have qutrits or more general qunits (systems with n different states) to be carried by photons. At first sight, this program does not seem to be very promising, because a photon, while carrying spin one, can be characterized as only a two-dimensional system, as it travels at the speed of light.

Yet, recently we were able to demonstrate that an individual photon can be prepared in eigenstates of external angular momentum carrying angular momentum of multiples of $\hbar$ and furthermore can also be prepared in superpositions of these eigenstates [15]. Also, we were able to demonstrate that in the process of parametric down-conversion, orbital angular momentum is conserved and we could show that, when two states are picked out, q-bit entanglement results [16].

In the present paper, we demonstrate for the first time entanglement of qutrits utilizing the orbital angular momentum of photons. This is done by selecting three values of the orbital angular momentum $(0, +\hbar, -\hbar)$, denoting the outcomes by 0, 1, and 2, respectively, for each photon, and demonstrating that the resulting entangled state violates a generalized Bell inequality for qutrits [17]. Orbital angular momentum states of photons are described in cylindrical coordinates by means of Laguerre Gaussian modes (LG_{pl}) which possess a helical structure of the wave front and a phase singularity. The index l is referred to as the winding number and p is the number of nonaxial radial nodes. Here we consider only cases of $p = 0$. The customary Gaussian mode can be viewed as an LG mode with $l = 0$. The handedness of the helical wave fronts of the LG modes is linked to the sign of the index l and can be chosen by convention. LG beams with an index l carry an orbital angular momentum of $l\hbar$ per photon [18–20].

There are several ways of producing LG modes out of the fundamental Gaussian beam. One simple method is to use a computer generated hologram which is a transmission phase grating with one dislocation in the center [21,22]. An incoming beam passing through the center of such a hologram is diffracted by the grating, and because of the dislocation the nth diffraction order becomes an LG mode with an index $l = n$. Our holograms were 3×3 mm in size, made on quartz glass with a periodicity of 30 μm, and had a diffraction efficiency of about 80% at 702 nm [23].

As already demonstrated in previous works experimentally [16] and confirmed theoretically [24] spontaneous parametric down-conversion conserves the photon orbital angular momentum. Beyond it the two photon state is not just a mixture but a coherent superposition of product states of the various Gaussian and LG modes [16]. In order to prove the entanglement of the orbital angular momentum experimentally, a prerequisite is to have

experimental techniques for preparing and analyzing superpositions of different orbital angular momentum eigenstates. It was shown that as long as one restricts itself to orbital angular momentum eigenstates with indices $l = -1, 0, 1$ a convenient method for creating superposition modes is to use a displaced hologram [15]. Although the mode decomposition after a displaced hologram [25] clearly shows that the output beam consists of many modes having different $p-$ and $l-$ index values, major contributions to the output beam are done by the LG_{00} and the LG_{01} modes for a hologram having one dislocation. Using this method arbitrary superpositions of two orthogonal modes can be produced where the two displacement parameters of the hologram in the transversal plane correspond to the two parameters identifying a certain superposition of two modes, their amplitude ratio, and their relative phase.

Our experimental setup is shown in Fig. 1. As a down-conversion source for the orbital angular momentum entangled photons we used a 1.5-mm-thick BBO (β-barium borate) crystal cut for type-I phase matching (that is, both down-converted photons carry the same linear polarization) which was pumped by an argon-ion laser at 351 nm with 120 mW light power. The crystal cut was chosen so as to produce down-converted photons at a wavelength of 702 nm at an angle of 4° off the pump direction.

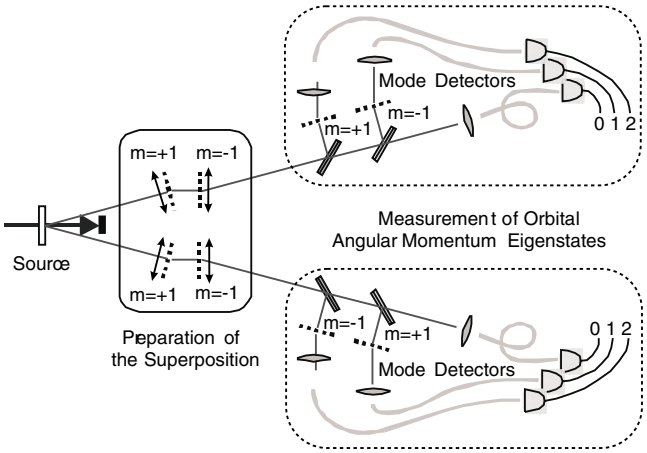

FIG. 1. Principle of the experimental setup. The *UV* beam at $\lambda = 351$ nm pumps a BBO crystal set for type-I phase matching. This results in spontaneous production of an entangled photon pair. In the measurement stages, the angular momentum correlations are observed by having on each side detectors able to measure photons with 0, $+\hbar$, and $-\hbar$ angular momentum, respectively. The corresponding outcomes are denoted as 0, 1, and 2 for the lower detection unit and 0, 2, and 1 for the upper detection unit. The coincidence logic identifies pairwise coincidences between the detectors on each side. The preparation stage allows one to prepare superposition of the eigenstates. This preparation stage generalizes the polarization rotator for linear polarization while the detector corresponds to a probabilistic polarization analyzer.

After parametric down-conversion each of the down-converted beams was sent through a holographic module consisting of two displaced holograms. The first hologram can transfer an incoming mode into superpositions of an LG_{01} and an LG_{00} mode, the second one into those of an LG_{0-1} and an LG_{00} mode [15,25]. These modules which can be viewed as generalizations of the polarizers in a polarization based two-dimensional Bell inequality experiment [26] can perform with their four moving axes (one horizontal and one vertical axis each) general rotations in the three-dimensional Hilbert space spanned by the orbital angular momentum eigenstates LG_{00}, LG_{01}, and LG_{0-1}. That is, any chosen displacement set of the holograms of each module projects the down-converted photons of that side onto a specific superposition of the LG_{00}, LG_{01}, and LG_{0-1} modes with a certain amplitude and relative phases.

Each photon then enters a mode detector designed to identify the angular momentum eigenstates LG_{00}, LG_{01}, and LG_{0-1}. The beam splitters, the first one with a splitting ratio 1:2 and the second one with 1:1, deflect the down-converted beams of each arm to mode detectors projecting an incoming photon onto an LG_{00}, an LG_{01}, or an LG_{0-1} mode, each with probability $\frac{1}{3}$. These outputs are indicated as 0, 1, and 2, respectively. The detector for the LG_{0-1} (the LG_{01}) mode consists of a hologram transforming the incoming LG_{0-1}, LG_{01} mode into the LG_{00} (Gaussian) mode and of a monomode optical fiber. Since the LG_{00} mode has the smallest spatial extension compared to all other LG modes, only it can be coupled into the monomode optical fiber. Therefore detecting a photon in the optical fibers of the mode detectors projects the incoming state onto an LG_{0-1} or LG_{01} mode, respectively. For projecting onto the LG_{00} mode the incoming photon was directly coupled into the monomode fiber without being sent through a hologram beforehand. This part of the setup can be seen as an analogue to the polarizing beam splitters in a Bell inequality experiment for polarization entangled photons. It can be viewed as a probabilistic "mode splitter." As has been shown experimentally [27,28] there also exist deterministic mode sorters which in principle would also be suitable for this application. However, the experimental setup would have become too complicated. Therefore since our count rates were such that we could afford some losses, the use of the "probabilistic mode splitter" seemed to be the most reasonable choice.

All nine possible combinations of coincidences for the three detectors on each side were measured using single-photon detectors, while a scanning program via step motors controlled the horizontal displacements of the holographic modules. Within the scan range of 1.5 mm, 16 equidistant positions of each hologram were chosen, resulting in a total number of 16^4 configurations.

Typical count rates were about 4500 s^{-1} for the coincidences and about 150 000 s^{-1} for the single counts,

which means an overall detection efficiency of 3%. This result is also in reasonable agreement with the overall collection efficiency if taking into account Fresnel losses at all optical surfaces ($\sim 95\%$ transmission), imperfect coupling into optical fibers ($\sim 70\%$ for a Gaussian beam), nonideal interference filters ($\sim 75\%$ center transmission), the diffraction efficiency of the holograms ($\sim 80\%$), and the efficiency of the detectors ($\sim 30\%$).

In order to demonstrate that the correlation observed cannot be explained by local realistic models we made use of a generalized type of Clauser-Horne-Shimony-Holt (CHSH) Bell inequalities [29] introduced by Collins *et al.* In their work [17] they give an explicit term I_3 for the special case of a three-dimensional entangled system with $I_3 \leq 2$ for local realistic models. However, in analogy to the usual CHSH Bell's inequality we will denote I_3 as S_3 which is given by

$$\begin{aligned} S_3 = &+ P(A_1 = B_1) + P(B_1 = A_2 + 1) + P(A_2 = B_2) \\ &+ P(B_2 = A_1) - P(A_1 = B_1 - 1) - P(B_1 = A_2) \\ &- P(A_2 = B_2 - 1) - P(B_2 = A_1 - 1), \end{aligned} \quad (1)$$

where

$$P(A_a = B_b + k) = \sum_{j=0}^{2} P(A_a = j, B_b = j + k \mathrm{mod} 3) \quad (2)$$

denote the probabilities of the joint measurements on both sides. A_1, A_2 and B_1, B_2 denote two possible settings of the local analyzers on each side. Measurements in a three-dimensional entangled system have three possible outcomes denoted by 0, 1, or 2. Each of the settings A_1, A_2 and B_1, B_2 corresponds experimentally to a specific configuration of the holograms of a holographic module. For certain choices of the local analyzers, the conflict between the local realistic models and quantum mechanics becomes maximal. For maximally entangled states the quantum prediction yields $S_3(\max) = 4/6\sqrt{3} - 9 \simeq 2873$.

As mentioned above, many different settings for the local analyzers were realized in our experiment by sequential scanning of the two holograms of each module. Their actual positions represent a possible setting of the local analyzer A_i or B_j, respectively. After performing the measurement, the probability $P(A_i, B_j)$ for a joint measurement between the outcome m on the one side and the outcome n on the other side, with $m, n = 0, 1, 2$ was calculated. This was done for a given set of A_i, B_j by dividing the number of coincidences $C_{m,n}$, between the detector with the outcome m and the detector with the outcome n, by the total number of coincidences. The measurement time was 2 s for each setting of the local analyzers. For about 21.5×10^6 quadruples $(A_1, A_2; B_1, B_2)$ the expression S_3 was calculated. The sorted distribution of the values violating the three-dimensional CHSH Bell inequality is shown in Fig. 2. For about 35 000 quadruples S_3 was greater than 2 with

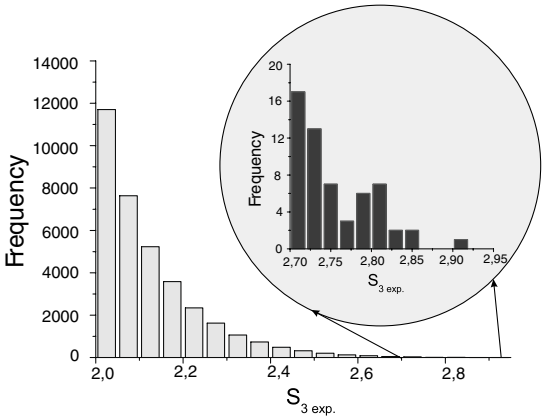

FIG. 2. Two-photon, two-qutrit violations of a Bell-type inequality. The graph shows the frequency with which a violation of the generalized CHSH Bell inequality was observed. The upper limit for the correlation parameter for local realistic theories is 2.0. The inset shows the violations close to the theoretical quantum upper limit. The numbers should be compared with the total number of 16^4 measured correlations altogether observed.

the maximum of $S_3(\max_{\mathrm{exp}}) = 2.9045 \pm 0.0517$ which means a violation by more than 18 standard deviations. The errors were calculated assuming Poisson statistics. In Fig. 2 the envelope of the bars can be regarded as a measure for the frequency distribution of the values contradicting local realism.

It is known [30] that the threshold for maximally entangled states not violating a Bell's inequality drops when one goes to higher dimensions. In our experiment by measuring the coincidence rates for the zero setting of the holographic modules, we could calculate the amplitudes of the three-dimensional orbital angular momentum entangled state. Denoting a state represented by the coincidence measurement of a photon at the output m and a photon at the output n by $|m, n\rangle$ we found the state yielding to the above violation was given by

$$\psi = 0.65|0, 0\rangle + 0.60|1, 1\rangle + 0.47|2, 2\rangle. \quad (3)$$

Although the state (3) is not a maximal entangled state, the greatest violation of the Bell's inequality achieved with this state experimentally $S_3(\max_{\mathrm{exp}})$ is very close to the maximum possible value $S_3(\max)$.

As theoretically shown [30], one of the important aspects of higher dimensional entangled states is that they are more resistant to noise. This fact makes long-distance quantum communication, which usually suffers from the noisy channels, more feasible when using qunits instead of qubits.

One major application for higher dimensional entangled states is quantum cryptography with higher alphabets [10,11]. In contrast to the usual two-dimensional cryptography protocols [31] where the message is encoded in a binary way via the two eigenstates of the system, in a

three-dimensional quantum cryptography scheme, for example, the key would be a string with three possibilities for each element (0, 1, and 2). Therefore the message is encoded via a three level system. This allows one to increase the flux of information. An experimental demonstration of multilevel quantum cryptography can be realized utilizing photon's orbital angular momentum. In order to perform quantum key distribution, one can use our existing setup. By making the two holographic modules switch randomly between two settings and recording the coincidences, a common key can be established between two parties.

Given the multilevel quantum cryptography as an example, it is to be expected that higher dimensional entanglement will be useful in quantum communication systems and may even lead to novel developments.

This work was supported by the Austrian FWF, Project No. F1506.

[1] S. L. Braunstein, A. Mann, and M. Revzen, Phys. Rev. Lett. **68**, 3259 (1992).
[2] Ch. H. Bennett, G. Brassard, and A. K. Ekert, Sci. Am. **267**, No. 4, 50–57 (1992).
[3] Charles H. Bennett, Gilles Brassard, Claude Crépeau, Richard Jozsa, Asher Peres, and William K. Wootters, Phys. Rev. Lett. **70**, 1895–1899 (1993).
[4] M. A. Nielsen and I. L. Chuang, *Quantum Information and Quantum Communication* (Cambridge University Press, Cambridge, U.K., 2000).
[5] C. A. Sackett, D. Kielpinski, B. E. King, C. Langer, V. Meyer, C. J. Myatt, M. Rowe, Q. A. Turchette, W. B. Itano, D. J. Wineland, and C. Monroe, Nature (London) **404**, 256–259 (2000).
[6] Arno Rauschenbeutel, Gilles Nogues, Stefano Osnaghi, Patrice Bertet, Michel Brune, Jean-Michel Raimond, and Serge Haroche, Science **288**, 2024–2028 (2000).
[7] J.-W Pan, D. Bouwmeester, M. Daniell, H. Weinfurter, and A. Zeilinger, Nature (London) **403**, 515 (2000).
[8] J.-W Pan, M. Daniell, S. Gasparoni, G. Weihs, and A. Zeilinger, Phys. Rev. Lett. **86**, 4435–4438 (2001).
[9] John C. Howell, Antia Lamas-Linares, and Dik Bouwmeester, Phys. Rev. Lett. **88**, 030401 (2002).
[10] M. Bourennane, A. Karlsson, and G. Björk, Phys. Rev. A **64**, 012306 (2001).
[11] H. Bechmann-Pasquinucci and A. Peres, Phys. Rev. Lett. **85**, 3313 (2000).
[12] Andris Ambainis, quant-ph/0204022.
[13] S. Massar, quant-ph/0109008v3.
[14] J. D. Franson, Phys. Rev. Lett. **62**, 2205–2208 (1989).
[15] A. Vaziri, G. Weihs, and A. Zeilinger, J. Opt. B Quantum Semiclassical Opt. **4**, S47–S50 (2002).
[16] A. Mair, A. Vaziri, G. Weihs, and A. Zeilinger, Nature (London) **412**, 313 (2001).
[17] D. Collins, N. Gisin, N. Linden, S. Massar, and S. Popescu, Phys. Rev. Lett. **88**, 040404 (2002).
[18] L. Allen, M. W. Beijersbergen, R. J. C. Spreeuw, and J. P. Woerdman, Phys. Rev. A **45**, 8185–8189 (1992).
[19] H. He, M. E. Friese, N. R. Heckenberg, and H. Rubinsztein-Dunlop, Phys. Rev. Lett. **75**, 826–829 (1995).
[20] M. E. J. Friese, J. Enger, H. Rubinsztein-Dunlop, and N. R. Heckenberg, Phys. Rev. A **54**, 1593 (1996).
[21] V. Yu Bazhenov, M. V. Vasnetsov, and M. S. Soskin, JETP Lett. **52**, 429–432 (1990).
[22] J. Arlt, K. Dholakia, L. Allen, and M. J. Padgett, J. Mod. Opt. **45**, 1231–1237 (1998).
[23] B. Kley (private communication).
[24] S. Franke-Arnold, S. M. Barnett, M. J. Padgett, and L. Allen, Phys. Rev. A **65**, 033823 (2002).
[25] M. Padgett, J. Courtial, L. Allen, S. Franke-Arnold, and S. M. Barnett, J. Mod. Opt. **49**, 777–785 (2002).
[26] G. Weihs, T. Jennewein, C. Simon, H. Weinfurter, and A. Zeilinger, Phys. Rev. Lett. **81**, 5039–5043 (1998).
[27] M. V. Vasnetsov, V. V. Slyusar, and M. S. Soskin, Quantum Electron. **31**, 464 (2001).
[28] J. Leach, M. J. Padgett, S. M. Barnett, S. Franke-Arnold, and J. Courtial, Phys. Rev. Lett. **88**, 257901 (2002).
[29] J. F. Clauser, M. A. Horne, A. Shimony, and R. A. Holt, Phys. Rev. Lett. **23**, 880–884 (1969).
[30] D. Kaszlikowski, P. Gnacinski, M. Zukowski, W. Miklaszewski, and A. Zeilinger, Phys. Rev. Lett. **85**, 4418 (2000).
[31] T. Jennewein, C. Simon, G. Weihs, H. Weinfurter, and A. Zeilinger, Phys. Rev. Lett. **84**, 4729–4732 (2000).